Design and experiment of a self-propelled two-row garlic combine harvester

Xu Zhang,[1,3] Hua Li,[2,3] Xindan Qi,[1,3] Samuel Mbugua Nyambura,[2,3] Yongjian Wang,[2,3] Jieyi Fu[2,3]

[1]College of Mechanical and Power Engineering, Nanjing Tech University, Nanjing; [2]College of Engineering, Nanjing Agricultural University, Nanjing; [3]Key Laboratory of Intelligent Agricultural Equipment in Jiangsu Province, Nanjing Agricultural University, Nanjing, China

Abstract

Given the significant damage rate observed during the transportation of current garlic combine harvesters in China, this study aims to design a new garlic combine harvester capable of achieving minimal harvest losses. The designed machine can simultaneously complete operations for garlic digging, clamping transport, seedling-bulb separation, soil cleaning, and fruit collection across two rows. Through the use of theoretical analysis and calculation of garlic harvesting operations, the key parameters of soil-breaking device, clamping transport device, length-limiting cutting device, and soil cleaning conveyor were determined. The Box-Behnken test technique was utilized within Design-Expert software, and orthogonal experiments were conducted with the unit's forward speed, digging depth, and soil-breaking angle as test factors, and the stem cutting rate and bulb damage rate as test indices. The test results showed that when the unit's forward speed, digging depth, and soil-breaking angle were 0.49 m/s, 100 mm, and 20°, respectively, the working parameter combination was the best, and the rate of stem cutting and damage were 95.71% and 3.10%, respectively. The findings from the field experiment and optimization aligned closely. This study can provide reference for the development of mechanized garlic harvesting.

Correspondence: Hua Li, Key Laboratory of Intelligent Agricultural Equipment in Jiangsu Province, Nanjing Agricultural University, Nanjing, China. E-mail: lihua@njau.edu.cn

Key words: garlic harvester; flexible clamping; seedling-bulb separation; soil cleaning; parameter optimization.

Contributions: all the authors made a substantive intellectual contribution, read and approved the final version of the manuscript and agreed to be accountable for all aspects of the work.

Conflict of interest: the authors declare that they have no competing interests, and all authors confirm accuracy.

Acknowledgments: this study was funded by the Garlic Mechanized Intelligent Operation Research and green production technology promotion.

Received: 5 December 2023.
Accepted: 13 July 2024.

Journal of Agricultural Engineering 2025; LVI:1676
doi:10.4081/jae.2024.1676

Introduction

Garlic is a renowned edible and medicinal plant, serving as an important economic crop in China (Li *et al*., 2020; Yu *et al*., 2023). In 2020, China's garlic production accounted for 74% of the world's total output. It is widely cultivated in Jinxiang of Shandong Province, Pizhou of Jiangsu Province, and Qi county of Henan Province (Zhao, 2023). China has developed a relatively advanced industrial chain for garlic production and is the world's largest producer and exporter of garlic (Yu *et al*., 2015). Currently, garlic harvesting in China mainly relies on manual excavation using flat shovels, resulting in low efficiency that cannot meet the requirements for rapid and efficient modern agricultural mechanization (Sun *et al*., 2018; Zhu *et al*., 2022; Yu *et al*., 2013). Therefore, it is of great practical significance to develop a reliable and efficient garlic harvester.

In order to improve the harvest level of garlic mechanization, domestic and foreign scholars have done a lot of research. According to the harvesting method, the existing harvesters can be divided into segmented and combined harvesters (Fan *et al*., 2022). The garlic harvester of the Top Air company in the United States is mainly based on piecework harvesting. The company's product GW 4400 garlic digging and laying machine can excavate 4 rows of garlic and separate part of garlic from soil. The machine needs to work with the garlic picker, and is not suitable for wet soil (Qin *et al*., 2019). The 4S-1200 garlic harvester of Weifang Aotian Agricultural Packaging production belongs to the combined shovel chain garlic harvester, which has simple structure and wide application range, but it requires a large amount of labor in the later period (Hu *et al*., 2007). ERME's third-generation bundled garlic harvester RL3 can dig, clamp, cut and collect garlic in three rows by hanging at three points behind the powered tractor (Zhao *et al*., 2020; Yu *et al*., 2021). Hou *et al*. (2021a, 2021b) designed a hand-held double-row garlic combine harvester, which could realize posture correction, gripping, cutting and garlic collection of garlic plants, but the maximum working speed was only 0.74m·s^{-1}. Although foreign garlic harvesters are generally advanced, they have large row spacing and cannot adapt to the garlic harvesting under the Chinese row spacing planting mode (Zhang *et al*., 2023; Zhu *et al*., 2023). The typical problems of existing domestic garlic combine harvesters are poor applicability and high garlic damage rate (Xing *et al*., 2012; Sun *et al*., 2019).

In order to solve the problem of high damage rate of existing garlic harvesters, a self-propelled two-row garlic combine harvester was designed based on the agronomy of garlic planting in China. At present, there are much research on garlic harvesters in China. Compared with segmented and hand-held harvesters, this machine has the advantage of high harvesting efficiency. Compared with more rows of combine harvesters, this machine has the advantages of light structure, low loss harvest. The machine can complete the operations of garlic digging, clamping transport, seedling-bulb separation, soil cleaning and fruit collection. The prototype was manufactured, and the field harvest test was carried out, and the optimal working parameters were determined. The research and development of this machine can provide reference for the structure improvement and operation performance optimization of self-propelled garlic combine harvester.

Materials and Methods

Overall structure and working principle

In order to adapt to the garlic planting pattern in China, a self-propelled two-row garlic harvester was designed, and the overall structural design of the harvester is shown in Figure 1. It is mainly composed of a track chassis walking device, a digging device, a flexible clamping transport device, a length-limiting cutting device, and a soil cleaning conveyor.

During the operation, the garlic plants were shunted by the seedlings gathering rods. After loosening of the soil was completed by the digging device, the garlic seedlings were transferred to the clamping transport device. Here, they were uplifted and moved diagonally upwards. When the garlic seedlings reached the length-limiting cutting device, the bulbs came into proximity with the garlic stem-limiting rods, thereby causing the garlic seedlings to be securely gripped by the clamping transport device. The garlic seedlings and bulbs were then separated by two blades. The cut garlic seedlings fell freely into the field after being transported for some distance, and the bulbs fell on the rod-type chain of the soil cleaning conveyor for partial soil removal. These were finally transported to the bulbs collection box through the chain to complete the harvest operation. The main technical parameters of the combine are shown in Table 1.

Design and parameter determination of key components

Soil-breaking device

The soil-breaking device mainly functions to loosen the soil during operation, which mainly consists of a soil-breaking shovel, digging depth adjustment plate, and angle adjustment plate, as shown in Figure 2. The main parameters affecting the performance

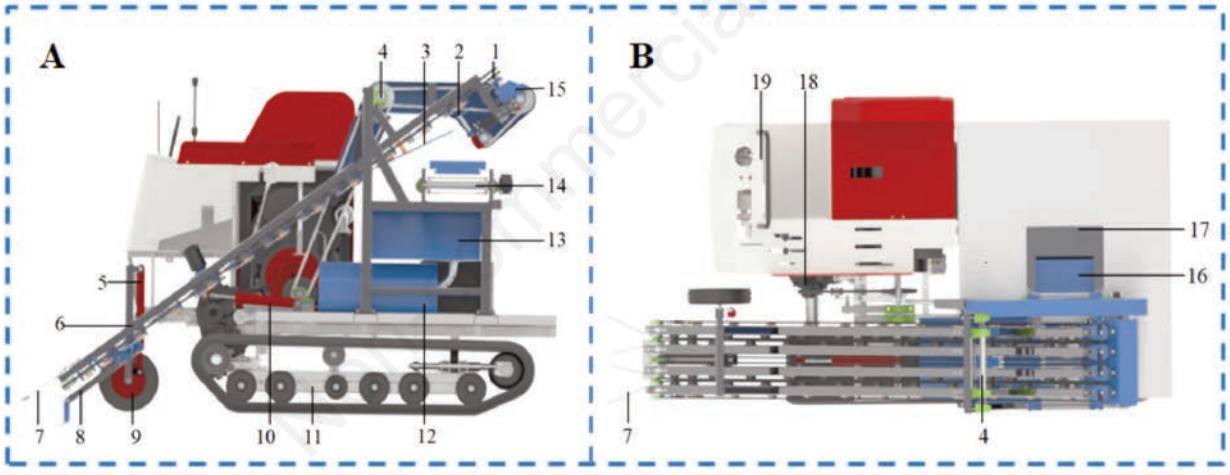

Figure 1. Structure of garlic combine harvester. Side (A) and top (B) view. (1) Active pulley; (2) cutter; (3) length-limiting cutting device; (4) hinged shaft; (5) depth limiting hydraulic cylinder, (6) clamping transport device; (7) seedlings gathering rods; (8) digging device; (9) depth limiting wheel; (10) lifting hydraulic cylinder; (11) crawler chassis; (12) fuel tank; (13) soil slide plate; (14) soil cleaning conveyor; (15) gear box; (16) garlic slide plate, (17) bulbs collection box; (18) output spindle; (19) operation table.

Table 1. Technical parameters of self-propelled two-row garlic combine harvester.

Structural parameters	Value
Overall dimensions (length × width × height) /mm	2880×1570×1950
Output power (diesel engine) /kw	16.2
Output speed (diesel engine) /(r /min^{-1})	2200
Travel speed /(m /s^{-1}) (stepless speed regulation)	0~1.5
Harvested rows	2
Harvest row spacing /mm	200
Digging depth /mm	80~120

of the soil-breaking device were the width of the shovel, soil-breaking angle, and digging depth. Among them, the digging depth was dependent on the average growth depth of garlic. In order to effectively break the soil and avoid injuring the garlic, the digging depth was greater than the maximum growth depth of garlic. The device could adjust the digging depth within the range of 80~120 mm through the assembly of different pore sizes on the digging depth adjustment plate.

The parameters for determining the shovel width were based on the garlic planting row spacing and the structural position of the soil-breaking device in the harvester. To maintain shovel rigidity against soil resistance, a rectangular design was adopted for the shovel within the device. Considering the need to work on two lines simultaneously during operation and to ensure effective soil loosening without leakage or digging, the shovel width B should adhere to the following relation (Hou *et al*., 2020) :

$$B = m + 2r + \mu \quad (1)$$

where m is garlic row spacing, mm. Notably, m=200 mm according to the agronomy of Xuzhou area; r is the radius of the garlic, mm, and r=25 based on field measurements; μ is the path deviation of the machine, mm, where μ is taken to be 50 mm. According to the relation, the width of the digging shovel was 300 mm.

The soil-breaking angle of shovel is an important parameter which affects the performance of excavation. From Figure 3, it can be deduced from the stress analysis diagram of the shovel that the following conditions should be met to successfully excavate garlic (Hou *et al*., 2021):

$$P\cos\alpha - T - G\sin\alpha \geqslant 0 \quad (2)$$

$$F - P\sin\alpha - G\cos\alpha \geqslant 0 \quad (3)$$

where P is the force of the shovel lifting the soil, N; T is the friction between soil and the surface of shovel ($T = f F$), where f =tanϕ. f is the friction coefficient between the soil and the shovel, and ϕ is the friction angle between the soil and the shovel, generally

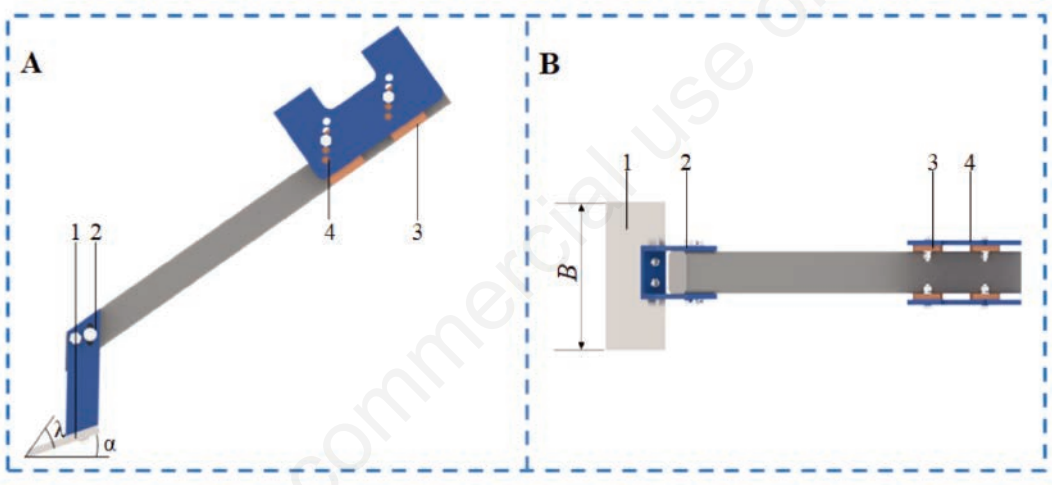

Figure 2. Structure diagram of soil-breaking device. Side (**A**) and top (**B**) view. (1) Soil-breaking shovel; (2) angle adjustment plate; (3) fixed plate; (4) digging depth adjustment plate.

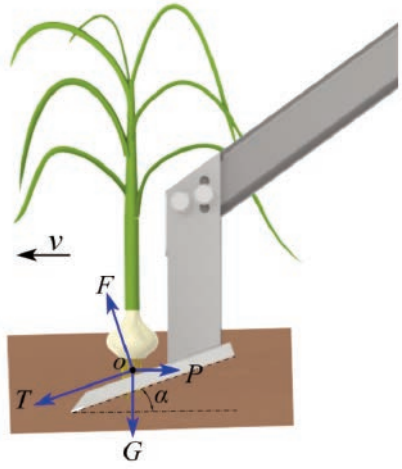

Figure 3. Stress analysis diagram of digging shovel.

30~36°, N; F is the reaction force of shovel against soil, N; G is the weight of the soil being dug up.

Equations (2) and (3) can be further analyzed to derive the following equation:

$$\alpha \leqslant arctan\frac{P\text{-}fG}{fP+G} \quad (4)$$

According to Equation (4), the excavation resistance was directly proportional to the soil-breaking angle α of the shovel. A smaller soil breaking angle α lead to reduced excavation resistance, thus improving the shovel's excavation performance. However, when the length of the shovel surface is fixed, the digging depth will be reduced, which is easy to cause bulb damage and incomplete soil breaking. Conversely, if the angle α is too large, the digging depth will increase, thereby reducing the rate of bulb damage, but increasing the soil resistance on the shovel. This, in turn, leads to higher energy consumption for the entire machine and increased wear on the shovel. Considering the different soil conditions of planting garlic in different regions, the soil-breaking angle was generally designed to be 15~30°, and the device design could achieve soil-breaking angle of 15, 20 and 25° through adjustment.

Flexible clamping transport device

To minimize clamping damage during transportation, the flexible clamping transport device utilized a B-type triangular belt made of soft rubber to grip the conveyor belt, as shown in Figure 4. When the clamping transport device secured the garlic seedling, the soil was initially loosened by the soil-breaking shovel, thereby causing the garlic seedling to tip backward towards the machine, as shown in Figure 5. The conveying speed of the clamping transport device is an important parameter influencing the harvesting operation. As per the schematic diagram of the garlic extraction process, the relationship between the clamping transport speed and the forward direction of the unit is illustrated as follows:

$$\frac{V_r}{\sin\lambda} = \frac{V_m}{\sin(180^\circ\text{-}\lambda\text{-}\beta)} \quad (5)$$

$$\lambda = 90^\circ + \theta \quad (6)$$

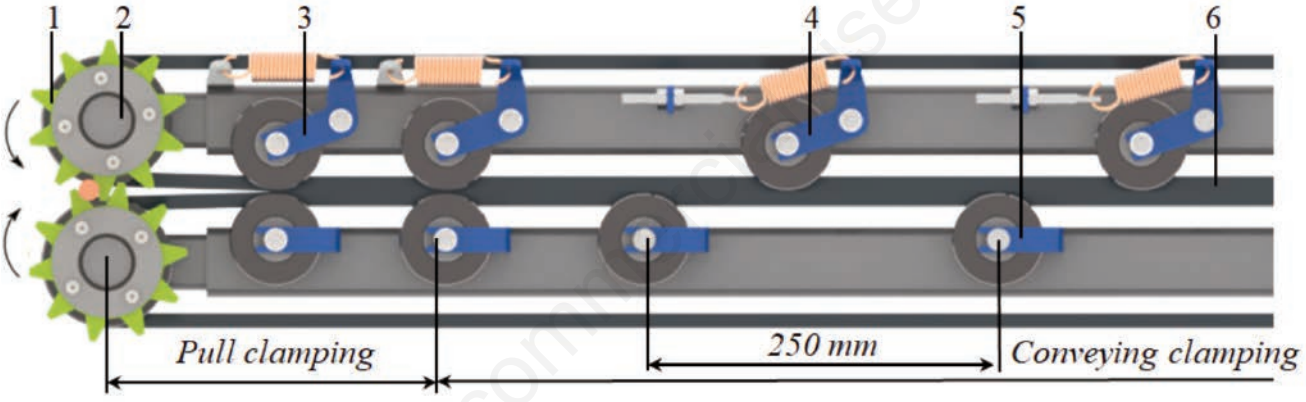

Figure 4. Structure diagram of flexible clamping transport device. (1) Rubber dial; (2) driven pulley; (3) type I tension wheel; (4) type II tension wheel; (5) type III tension wheel; (6) belt.

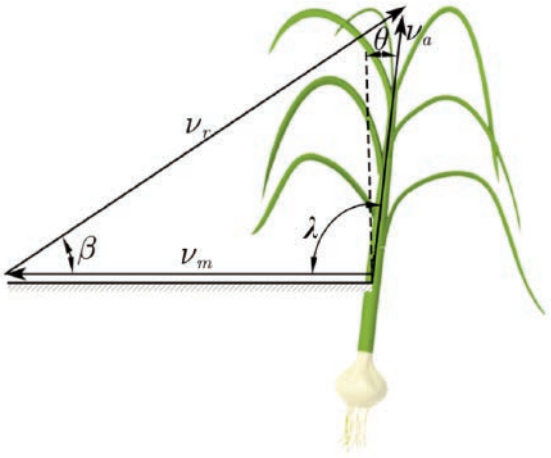

Figure 5. Schematic diagram of garlic extraction process.

where v_r is the flexible clamping transport belt speed, ms^{-1}; v_m is the machine forward advance speed, ms^{-1}; λ is the angle between the absolute speed of the flexible clamping conveyor belt and the forward speed of the machine, (°); β is the inclination angle of the flexible clamping transport device, (°); θ is the garlic pouring angle, (°), whereby the value is 5° ~ 10° (Wang *et al*., 2012).

By inserting formula (6) into (5):

$$V_r = \frac{\cos\theta}{\cos(\beta+\theta)} V_m \quad (7)$$

It can be seen from Equation (7) that the speed of the flexible clamping transport device was linearly related to the forward speed of the machine (Hou *et al*, 2022; Hou *et al*, 2023). The angle β of the clamping transport device was adjusted by lifting the hydraulic cylinder, with the value of β also accounting for the layout of the entire machine structure. Combining the above factors and taking β=36°, then v_r= (1.32 ~ 1.42) v_m.

As depicted in Figure 6, the tensioning wheel of the flexible clamping transport device designed by this machine was classified into three categories based on its functions. The tensioning wheel was axially constrained by a fixed shaft and nut. Types I and II tensioning wheels were considered floating wheels, with the wheel body and swing arm capable of rotating around the fixed shaft. Depending on the operating conditions, the type II tension wheel was adjusted to the desired clamping force by stretching the spring using a tensioning screw. The center distance between tensioning wheel on the same side of the clamping track was 250 mm.

Length-limiting cutting device

The separation of garlic seedlings from bulbs is a crucial aspect of garlic harvesting, as it determines the effectiveness of seedling-bulb separation and the length of the stem. The structure of the length-limiting cutting device is illustrated in Figure 7. This device regulates the stem length using a garlic stem limiting rod, thereby facilitating the separation of seedlings via a cutting knife positioned at the rear of the device. The length-limiting cutting device comprises of an adjustment plate, a fixing plate, and a garlic stem length-limiting rod. The device secures the garlic seedlings tightly through friction between the upper surface of the bulb and the lower surface of the garlic stem length limiting rod. The swift rotation of the cutting knife then separates the garlic seedling from the bulb. Additionally, the device allows for the adjustment of plant channel spacing by modifying the front and middle sections of the clamp adjustment plate, ensuring optimal fitting of the bulb's top to the garlic stem's length-limiting rod.

The parameters of length-limit cutting primarily encompass the angle of the stem-length limiting rod (ξ), the length of the stem length limiting rod (l), and the clamping height of the stem (h). The cutting process with limited length is depicted in Figure 8.

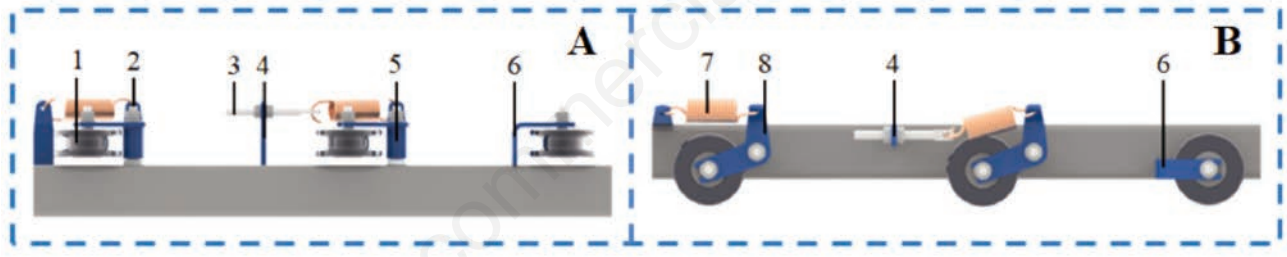

Figure 6. Structure diagram of tension wheel. Side (**A**) and upward (**B**) view. (1) Body of wheel body; (2) fixed shaft; (3) tensioning screw; (4) screw support plate; (5) shaft sleeve; (6) fixed wheel splint; (7) spring; (8) swing arm.

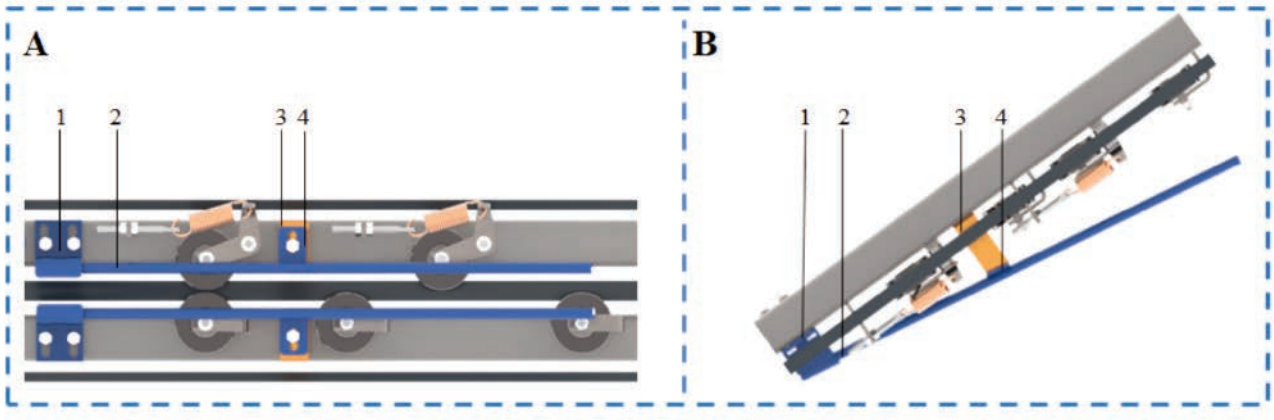

Figure 7. Structural diagram of length-limiting cutting device. Upward (**A**) and side (**B**) view. (1) Adjustment plate of front rod; (2) stem length limiting rod; (3) adjustment plate of middle rod; (4) fix plate of middle rod.

Excessively large angles (ξ) hinder plant posture adjustment and impede cutting efficacy. Conversely, smaller angles result in longer limiting rods, thereby impacting overall machine layout. Considering these factors, the angle between the stem-length limiting rod and the belt in this device was set at 10°. Ideally, when the plant reaches the cutting point, the upper surface of the garlic should just touch the stem-length limiting rod. Therefore, the length (l) of the garlic stem-limiting rod must satisfy the following relationship:

$$l=\frac{l_x}{\sin\xi}=\frac{h\sin(90^\circ-\beta)}{\sin\xi} \quad (8)$$

where h is the plant clamping height, h =100 mm; β is the angle between the forward direction of the harvester and the direction of garlic transport; l is the length of garlic stem, mm; ξ is the inclination angle of the stem limiting rod and the conveyor belt, °; l_x is the auxiliary hanging edge of the stem length limiting rod and the garlic transporting direction.

The effective length of garlic stem limiting rod l=466 mm was obtained.

Soil cleaning conveyor

The soil cleaning conveyor consists of sprockets, an anti-soil belt, a side baffle, an anti-soil plate, and rod-type chain, as illustrated in Figure 9. The rod-type chain comprises two chains multiple metal rods with a diameter of 6 mm. Following the separation of garlic seedlings and bulbs, the bulbs descended onto the chain. Through rotation of the chain and the vibration of the machine, friction causes soil adhering to the garlic roots to dislodge and fall off. The anti-soil plate and the PVC anti-soil belt, adjacent to the chain, effectively minimize contact between the agitated soil and the chain. To prevent garlic leakage while considering the average bulb diameter, the two metal grating bars are spaced 25.8 mm apart. Considering the number of harvesting rows and machinery arrangement, the chain's conveying distance is set at L=600 mm, with the soil cleaning device having a width (W) of 350 mm. Once cleared of soil, the garlic descends into the bulb collection box via the garlic slide plate, thereby completing the entire operation process.

Planting patterns and agronomic requirements

Garlic cultivation in China predominantly involves manual

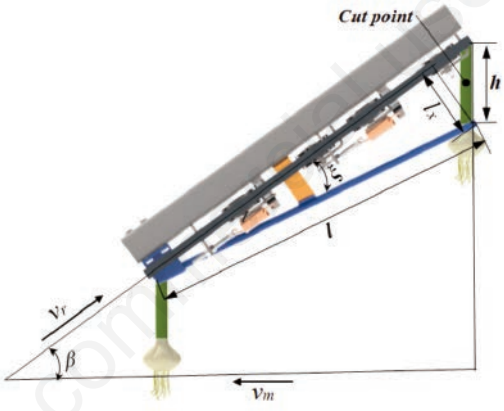

Figure 8. Schematic diagram of cutting positioning process.

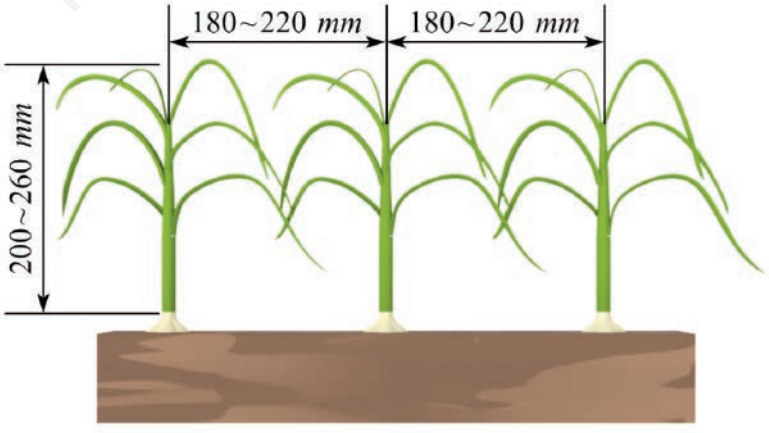

Figure 9. Structural diagram of soil cleaning conveyor. Side (**A**) and top (**B**) view. (1) Reducer; (2) drive sprocket; (3) anti-soil belt; (4) side baffle (5); anti-soil plate (6); rod-type chain; (7) motor.

planting, with varying techniques and no standardized approach. As shown in Figure 10, the unswept garlic plants typically exhibit heights ranging from 200 to 260 mm, with bulb diameters mainly falling between 50 to 60 mm. Stem diameters typically range from 13 to 17 mm, while row spacing commonly spans from 180 to 220 mm. Planting depth varies between 50 to 100 mm across different cultivation practices.

Test methods for prototype performance

Test standard

As there is still no standardized technical specification for garlic harvesting in China, this study utilizes the Shandong provincial local standard DB37/T2878.4-2016 "General Technical Requirements for Agricultural Harvest Machinery Part 4: Garlic Harvest Machinery" to assess the performance of the harvester. The garlic plants featured row spacing ranging from 180 to 220 mm, heights of 200 to 260 mm, bulb diameters of 50 to 60 mm, and planting depths of 50 to 90 mm.

Selection of test factors and indicators

The forward speed, digging depth, and soil breaking angle were selected as the test factors, while the bulb damage rate and stem cutting served as the evaluation metrics. Each experiment comprised 3 areas as an experimental unit, with each area measuring 3 meters in length. Following one trip of the prototype, the garlic within the experimental area was weighed, and the damaged garlic bulbs and the uncut garlic stems were individually weighed to calculate the garlic bulb damage rate and cutting rate. This process was repeated three times, and the collected data were averaged. The bulb damage rate represented the proportion of damaged bulbs in the harvest to the total experiment mass. The stem cutting rate indicated the ratio of the bulb mass meeting the specified stem length criterion (50~60 mm). The specific calculation formula is:

$$\eta_1=\frac{x_1}{x}\times100\% \quad (9)$$

$$\eta_2=\frac{x_2}{x}\times100\% \quad (10)$$

where η_1 is stem cutting rate, %; η_2 is bulb damage rate, %; x is total weight of garlic, kg; x_1 is garlic mass up to stem length, kg; x_2 is damaged garlic mass, kg.

Test scheme

Three-factor and three-level orthogonal experimental design was adopted, and the code of test factors is shown in Table 2.

Results and Discussion

Test results and parameter optimization

According to the actual operation requirements, experimental research was carried out on the forward speed, soil-breaking angle and digging depth, and the test scheme and results are shown in Table 3. The prototype and the field test diagram are shown in Figure 11A - details of the prototype - and Figure 11B - field test site and the garlic cutting effect.

Analysis of variance (ANOVA) was used to analyze the variance of the stem cutting rate and damage rate, and the results are shown in Table 4.

Table 2. Coding of test factor.

Code	Factor		
	Forward speed X_1 (ms^{-1})	Digging depth X_2 (mm)	Soil-breaking angle X_3 (°)
-1	0.35	90	15
0	0.55	100	20
1	0.75	110	25

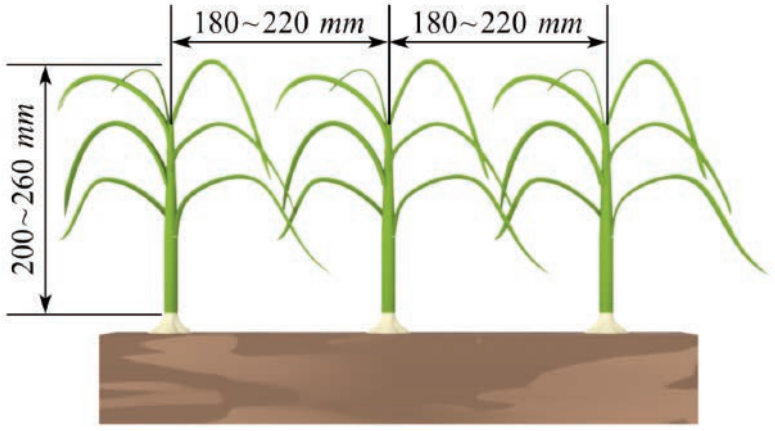

Figure 10. Garlic planting pattern.

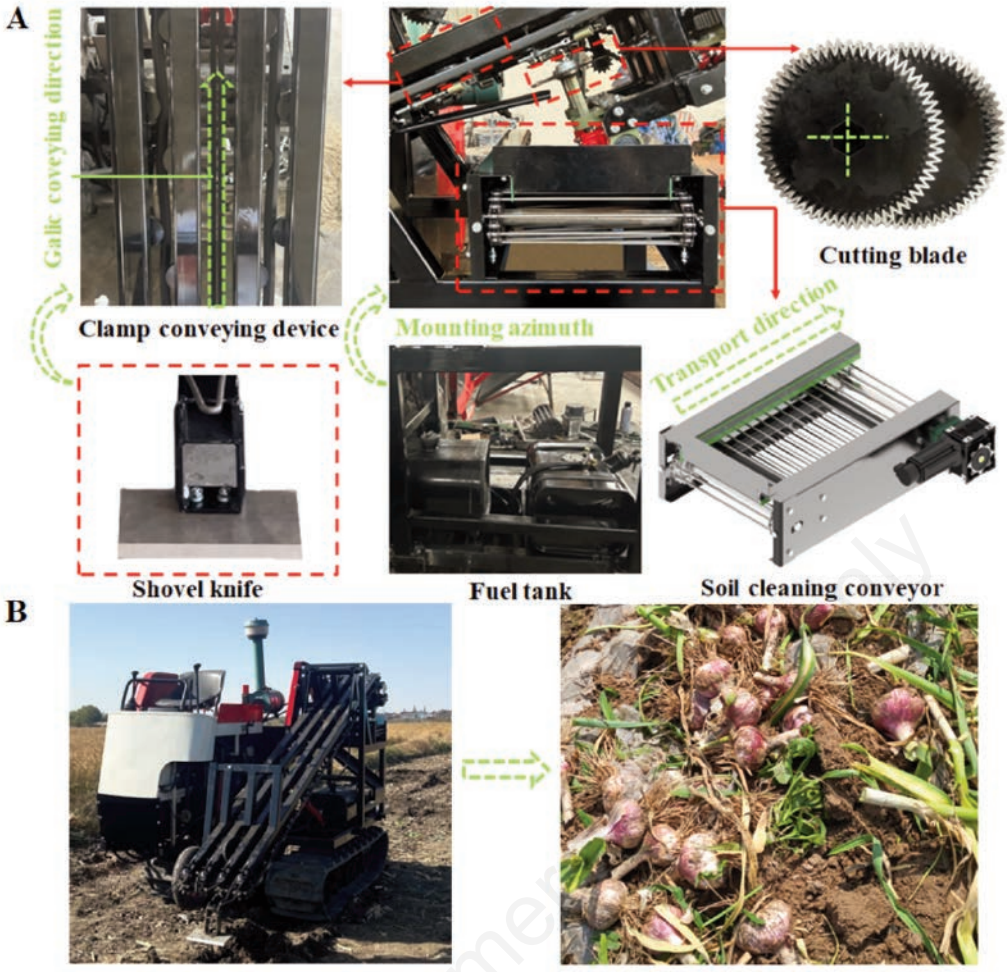

Figure 11. A) Prototype detail display. **B**) Field test diagram.

Table 3. Test scheme and results.

Number	Factor			Performance index	
	X_1	X_2	X_3	Stem cutting rate Y_1 (%)	Damage rate Y_2 (%)
1	-1	-1	0	92.57	2.79
2	1	-1	0	95.62	5.09
3	-1	1	0	90.59	2.22
4	1	1	0	93.47	5.06
5	-1	0	-1	91.92	3.12
6	1	0	-1	94..75	5.33
7	-1	0	1	92.03	2.72
8	1	0	1	95.08	4.98
9	0	-1	-1	96.28	4.81
10	0	1	-1	94.32	4.85
11	0	-1	1	96.32	4.57
12	0	1	1	94.41	4.51
13	0	0	0	96.13	3.31
14	0	0	0	95.89	3.29
15	0	0	0	97.28	3.56
16	0	0	0	95.79	3.34
17	0	0	0	96.38	3.67

Establishment of regression model and significance test

According to the experimental scheme and results in the table, multiple regression fitting analysis was conducted by using Design Expert 8.0.6.1 data analysis software to seek the optimal working parameters. As can be seen from Table 4, the *p*-values of the garlic stem cutting rate Y_1 and damage rate Y_2 models were both less than 0.01, indicating that the regression model was highly significant. The *p*-values of the lack of fit were all greater than 0.05, indicating that the regression model had a high degree of fit. The R^2 coefficients of determination were 0.9752 and 0.9861, respectively, indicating that the regression model could explain more than 97% of the sample data, and the regression model could be used to predict and analyze the stem cutting rate and damage rate of harvested garlic. According to the data analysis of the stem cutting rate Y_1, the coefficients of X_1, X_2, X_1^2 and X_2^2 were significant at the $p<0.05$

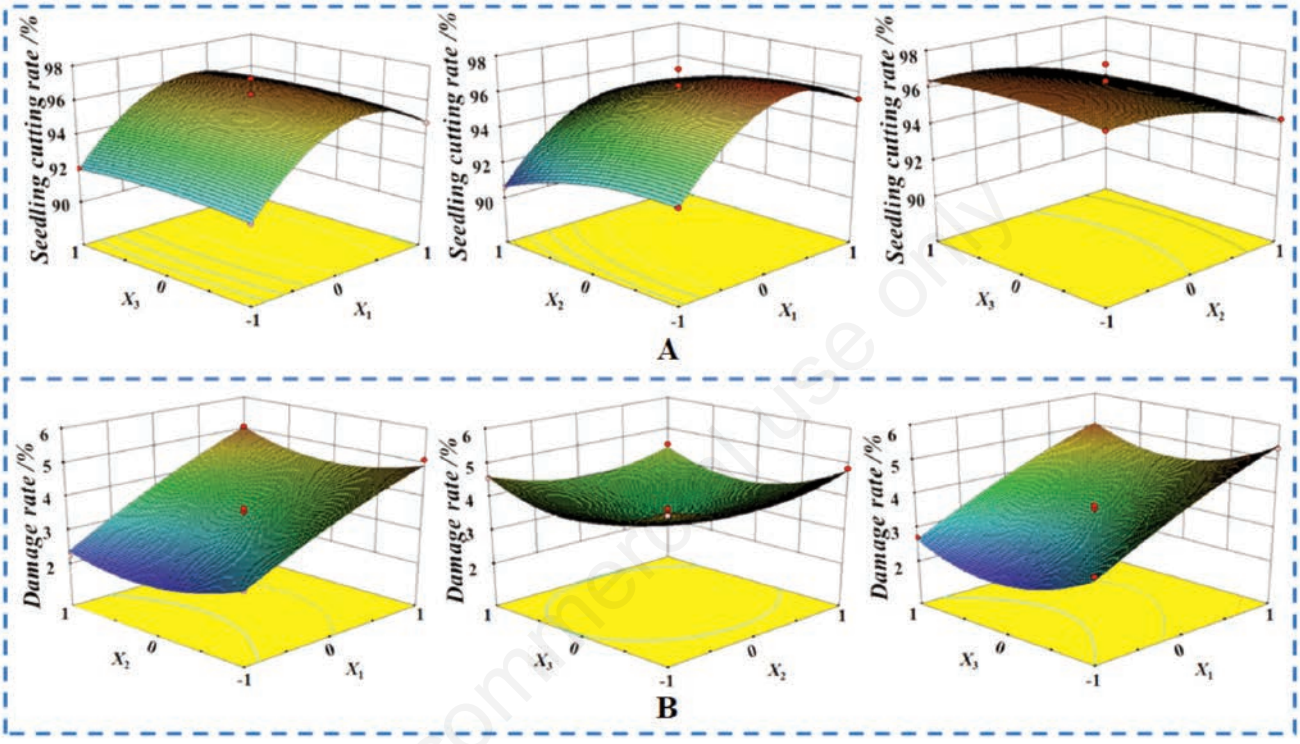

Figure 12. Response surface. **A**) Influence of interaction factors on the rate of cutting stem. **B**) Effect of interaction factors on damage rate.

Table 4. Variance analysis.

Source	Stem cutting rate Y1				Damage rate Y2			
	Sum of squares	Mean square	F	p	Sum of squares	Mean square	F	p
Model	56.76	6.31	30.56	<0.0001	15.51	1.72	55.28	<0.0001
X_1	17.43	17.43	84.49	<0.0001	11.54	11.54	370.18	<0.0001
X_2	8.00	8.00	38.77	0.0004	0.048	0.048	1.54	0.2545
X_3	0.041	0.041	0.20	0.6707	0.22	0.22	7.09	0.0323
X_1X_2	7.225×10^{-3}	7.225×10^{-3}	0.035	0.8569	0.073	0.073	2.34	0.1701
X_1X_3	0.012	0.012	0.059	0.8156	6.250×10^{-4}	6.250×10^{-4}	0.020	0.8914
X_2X_3	6.250×10^{-4}	6.250×10^{-4}	3.029×10^{-3}	0.9576	2.500×10^{-3}	2.500×10^{-3}	0.080	0.7853
X_1^2	27.58	27.58	133.67	< 0.0001	0.089	0.089	2.87	0.1342
X_2^2	1.90	1.90	9.21	0.0190	1.06	1.06	33.99	0.0006
X_3^2	0.35	0.35	1.71	0.2323	2.36	2.36	75.80	<0.0001
Residual	1.44	0.21			0.22	0.031		
Lack of fit	0.021	6.925×10^{-3}	0.019	0.995	0.10	0.034	1.16	0.4268
Pure error	1.42	0.36			0.12	0.029		
Sum	58.20				15.73			

level, while the rest were not. The order of significance of each factor on the garlic stem cutting rate was $X_1 > X_2 > X_3$. The data analysis of damage rate Y_2 showed that at the $p<0.05$ level, the coefficients of X_1, X_3 and X_2 were significant, while the rest were not. The order of significance of each factor on the damage rate of garlic was $X_1 > X_3 > X_2$. The regression models of stem cutting rate and damage rate were significant, but the lack of fit was not significant. After removing the non-significant variable terms, the regression equation was:

$$Y_1=96.29+1.48X_1-X_2+0.071X_3-0.043X_1X_2+0.055X_1X_3+0.013X_2X_3-2.56X_1^2-0.67X_2^2-0.29X_3^2 \quad (11)$$

$$Y_2=3.34+1.20X_1-0.077X_2-0.17X_3+0.13X_1X_2+0.013X_1X_3-0.025X_2X_3-0.15X_1^2+0.50X_2^2+0.75X_3^2 \quad (12)$$

To better understand the relationship between test indicators and factors, a 3D response surface diagram was constructed using Design-Expert software. This diagram aimed to elucidate the impact of different factors on both the stem cutting rate (Y_1) and damage rate (Y_2).

The response surface depicting the interaction of various factors is shown in Figure 12.

According to the response surface diagram illustrating the influence of interaction factors on the stem cutting rate, it is evident that as the machine's forward speed increased, the stem cutting rate initially increased and then decreased. This pattern arose due to the speed ratio between the cutting knife's rotational speed and the forward speed. A faster rotating cutter head facilitated smoother cutting of garlic stems. However, at higher forward speed, the plants experienced instability during transportation, leading to friction and collisions with the garlic stem length limiting rod led, thereby resulting in inaccurate positioning and reduced cutting rates. Moreover, an increase in digging depth, forward resistance, and machine vibration frequency may contribute to plant instability, further reducing the rate of stem cutting.

Regarding the damage rate, the response surface diagram reveals that higher machine forward speed correspond to elevated damage rates. This indicates that increased transport speed results in greater friction impact on garlic, thereby increasing the damage rate. Moreover, the damage rate initially decreased and then increased with the increase in digging depth and soil-breaking angle. This suggests that lower digging depths and soil-breaking angle bring the shovel closer to the bulbs, while higher values increase soil contact area, leading to soil accumulation and a higher risk of shovel damage to the bulb.

Using Design-Expert software, parameters were optimized within set constraints$\max Y_1$, $\min Y_2$; 0.35m/s $\le X_1 \le$ 0.75m/s, 90mm $\le X_2 \le$ 110mm, 15° $\le X_3 \le$ 25°, , resulting in an optimal parameter combination: machine forward speed of 0.49 m/s, digging depth of 98.1 mm, and soil-breaking angle of 20.54°. Predicted stem cutting rate and damage rate under these parameters were 95.82% and 3.11%, respectively. Adjusting these parameters to practical operability, the machine's forward speed, digging depth, and soil-braking angle were set to 0.49 m /s, 100 mm and 20°. This yielded a stem cutting rate of 95.71% and damage rate of 3.10%, aligning closely with test and optimization results. This met the criteria for high cutting rates and low damage rates of garlic combined harvest.

Conclusions

This paper presents the design of a self-propelled two-row garlic combine harvester capable of performing digging, clamping, conveying, seedling-bulb separation, soil cleaing, and garlic collection operations in a single pass. Key components such as the soil-breaking device, flexible clamping transport device, length-limiting cutting device, and soil cleaning conveyor were designed based on theoretical analysis and experimental validation.

A response surface regression model was developed using a Box-Behnken central composite design scheme, with garlic stem cutting rate and damage rate as evaluation indices. Through variance analysis and response surface analysis, the factors influencing garlic stem cutting rate were determined as follows: forward speed > digging depth > soil-breaking angle. For the damage rate of garlic, the factors influencing it were ranked as forward speed > soil-breaking angle > digging depth.

The Design-Expert 8.0.6.1 software was utilized to optimize and solve the established model, and the accuracy of the optimization results was validated through field experiments. The optimal working parameter combination was determined to be machine forward speed of 0.49 m/s, digging depth of 100 mm, and soil-breaking angle of 20°. Under these settings, the garlic cutting rate was measured at 95.71%, with a damage rate of 3.10%. Field tests confirmed that the harvester design effectively reduced garlic harvest damage and improved stem cutting rate, ultimately enhancing harvest efficiency and quality. This research contributes to the advancement of mechanized garlic harvesting in China and offers valuable insights for researchers and practitioners in the field.

References

Fan, J.B., Li, H., Fu, J.Y., Qi, X.D., Ding, Y.G. 2022. Design and Experiment of single-row garlic combine harvester. Acta Agr. Jiangxi 34:202-208.

Hou, J., Chen, Y., Li, Y., Li, G., Guo, H. 2021a. Design and experiment of shovel-screen combined green onion digging, shaking, and soil tillage device. Trans. CSAE 37:29-39.

Hou, J., Chen, Y., Li, Y., Wang, W., Li, G. 2020. Development of quantitatively-laying and self-propelled green onion combine harvesters. Trans. CSAE 36:22-33.

Hou, J., Li, C., Lou, W., Li, T., Li, Y., Zhou, K. 2022. Operation mechanism analysis and test of press root cutting device for garlic combine harvester. Trans. CSAE 53:167-174.

Hou, J., Li, C., Lou, W., Zhou, K., Li, Y., Li, T. 2023. Design and test of floating clamping device for garlic combine harvester. Trans. Chin. Soc. Agr. Machin. 54:137-145.

Hou, J., Li, C., Zhang, Z., Li, T., Li, Y., Wu, Y. 2021b. Design and test of double-row walking garlic combine harvester. Trans. CSAE 37:1-11.

Hu, Z.C., Wang, H.O., Wu, F., Hu, L.L. 2007. Summary of mechanized cultivation and processing of garlic in America. J. Anhui Agr. Sci. 13:4059-4061.

Li, SB, Li, H, Qi, XD, Li, B. H, Ding, Y.G. 2020. Research status and prospect of garlic harvester. Acta Agr. Jiangxi 32:99-104.

Qin, L.X. 2019. Research and Design of garlic combine harvester. University of Jinan.

Sun, H., Qiu, L.M. 2019. Design of sectional type garlic harvester. Agric. Equip. Veh. Eng. 57:90-92.

Sun, Q., Sui, Y.X., Zhao, L., Hou, J.L., Wang, C.Y., Cheng, Q., Shang, G., Jin, Y. 2018. Design and development of self-propelled garlic harvester. Agric. Res. 7:495-505.

Wang, J.S., Shang, S.Q. 2012. Development and experiment of double-row self-propelled carrots combine. Trans. CSAE 28: 38-43.

Xing, L.R., Li, R.X., Wang, T.X., Zhang, J. 2012. Design and analysis of split garlic harvester. Trans. Chin. Soc. Agr. Machin. 43:S137-40.

Yu, Z.Y., Hu, Z.C., Wang, H.O., Peng, B.L., Xie, H.X., Wu, F. 2013. Design and testing of head-stem segregation equipment for garlic. Trans. CSAE 29:7-15.

Yu, Z.Y., Hu, Z.C., Wang, H.O., Peng, B.L., Xie, H.X., Wu, F. 2015. Parameters optimization and experiment of garlic picking mechanism. Trans. CSAE 31:40-46.

Yu, Z.Y., Yang, K., Hu, Z.C., Peng, B.L., Gu, F.W., Yang, L., Yang M.J. 2023. Parameter optimization and simulation analysis of floating root cutting mechanism for garlic harvester. Comput. Electron. Agric. 204:107521.

Yu, Z.Y., Hu, Z.C., Yang, K., Peng, B.L., Zhang, Y.H., Yang, M.J. 2021. Operation mechanism analysis and parameter optimization of garlic root floating cutting device. Trans. Chin. Soc. Agr. Machin. 52:111-119.

Zhang, X.L., Qiu, L.Q., Sun, Q., Jing, Y.G., Zhao, Y., Yao, P.H. 2023. Design and test of a single-row harvesting and cutting integrated handheld garlic harvester. Appl. Sci. 13:7077.

Zhao, Z. 2023. Agricultural trade question: What is the current knowledge of garlic trade in China? World Agr. 1:139-140.

Zhao, D., Cai, D.M., Qin, L.X., Gao, X., Huang, W.T., Liu, C. 2020. Design and Experiment of modularized garlic combine harvester. Trans. Chin. Soc. Agr. Machin. 51:95-102.

Zhu, Z.B., Cheng, J.P., Wu, F., Hu, Z.C., Yu, Z.Y. 2023. Optimization of operation parameters of the garlic plant divider and lifter mechanisms. Agriculture (Basel) 13:189.

Zhu, Z.B., Li, W., Wen, F.J., Chen, L.Z., Xu, Y. 2022. Towards optimizing garlic combine harvester design with logistic regression. Appl. Sci. 12:6015.